Editors' Suggestion

Testing the Universality of Free Fall towards Dark Matter with Radio Pulsars

Lijing Shao,[1,*] Norbert Wex,[1] and Michael Kramer[1,2]
[1]Max-Planck-Institut für Radioastronomie, Auf dem Hügel 69, D-53121 Bonn, Germany
[2]Jodrell Bank Centre for Astrophysics, The University of Manchester, Oxford Road, Manchester M13 9PL, United Kingdom

(Received 29 March 2018; published 14 June 2018)

The violation of the weak equivalence principle (EP) in the gravitational field of Earth, described by the Eötvös parameter $\eta_\oplus$, was recently constrained to the level $|\eta_\oplus| \lesssim 10^{-14}$ by the *MICROSCOPE* space mission. The Eötvös parameter $\eta_{\rm DM}$, pertaining to the differential couplings of dark matter (DM) and ordinary matter, was only tested to the level $|\eta_{\rm DM}| \lesssim 10^{-5}$ by the Eöt-Wash group and lunar laser ranging. This test is limited by the EP-violating driving force in the solar neighborhood that is determined by the galactic distribution of DM. Here we propose a novel celestial experiment using the orbital dynamics from radio timing of binary pulsars, and obtain a competing limit on $\eta_{\rm DM}$ from a neutron-star–white-dwarf (NS-WD) system, PSR J1713 + 0747. The result benefits from the large material difference between the NS and the WD and the large gravitational binding energy of the NS. If we can discover a binary pulsar within ∼10 pc of the galactic center, where the driving force is much larger in the expected DM spike, precision timing will improve the test of the universality of free fall towards DM and constrain various proposed couplings of DM to the standard model by several orders of magnitude. Such a test probes the hypothesis that gravity is the only long-range interaction between DM and ordinary matter.

DOI: 10.1103/PhysRevLett.120.241104

Introduction.—In Ref. [1], Newton studied carefully the equivalence between mass and weight, which later became known as the equivalence principle (EP). It lies at the heart of Newtonian gravity, as well as Einstein's general relativity (GR) [2–5]. As emphasized by various authors [5–7], the EP should be treated as a heuristic concept, instead of a principle. Experimental examination of the EP started with pendulums by Galileo, Newton, Bessel, Potter *et al.* [5], and flourished with torsion balances by Eötvös, Dicke, Braginsky, and Adelberger *et al.* [3]. Recently, no violation was detected between titanium and platinum alloys from the first result of the *MICROSCOPE* satellite to the level $|\eta_\oplus^{(\rm Ti,Pt)}| \lesssim 10^{-14}$ [8], where the Eötvös parameter (with subscript denoting the attractor)

$$\eta_\oplus^{(A,B)} \equiv \frac{a_A - a_B}{\frac{1}{2}(a_A + a_B)}, \tag{1}$$

describes the difference in the acceleration of test bodies A and B in the gravitational field of Earth; in the following, we call the measurement of the numerator "precision" and the denominator the "driving force". The *MICROSCOPE* result surpasses the limits, by a factor of 10, from the Eöt-Wash group [3,9]. On the other hand, the Eötvös parameter towards the Sun was constrained to be $|\eta_\odot| \lesssim 10^{-13}$ by lunar laser ranging (LLR) [10] and the Eöt-Wash group [9]. The physical distinction between $\eta_\oplus$ and $\eta_\odot$ is necessary because, in the analysis, the driving forces are produced by different compositions of the attractor, mostly hydrogen (∼91.2%) and helium (∼8.7%) for the Sun, and iron (∼32.1%), oxygen (∼30.1%), silicon (∼15.1%), and magnesium (∼13.9%) for Earth. If the EP violation is caused by a long-range force mediated by a new massless (or ultralight) field, $\eta_\oplus$ and $\eta_\odot$ probe different aspects of its couplings between the attractor and test masses [3]. *MICROSCOPE* has no gain in the driving force from the Sun; thus, it does not improve the limit on $\eta_\odot$. The composition of two test masses is also important. It is related to the couplings between the force-mediating field and the force receivers. In this regard to the gravitational energy, a branch of well-motivated studies use self-gravitating bodies to probe the strong EP [2,4,11] with LLR [10] and pulsar timing experiments [12–19].

Stubbs [20] was the first to point out that the Eöt-Wash searches for EP violation also put limits on the Eötvös parameter $\eta_{\rm DM}$ when the dark matter (DM) acts as the attractor. It could originate from differential couplings between DM and ordinary matter [3,21]. With its actual ability in measuring differential acceleration worse than the Eöt-Wash group, *MICROSCOPE* benefits from a larger driving force, 7.9 $\rm m\,s^{-2}$ at 710 km altitude versus 1.68×10^{-2} $\rm m\,s^{-2}$ for the Eöt-Wash laboratory [8,9]. However, because of a much smaller driving force in the solar neighborhood from the DM, $a_{\rm DM} \simeq 10^{-10}$ $\rm m\,s^{-2}$ [22], previous studies were only able to constrain $|\eta_{\rm DM}| \lesssim 10^{-5}$ [9,23–29].

In this Letter, we demonstrate that the current limit in testing the EP from pulsars [12,14,17–19,30,31] is already

approaching the best available constraint on $\eta_{\rm DM}$. Considering (i) the neutron-rich composition of pulsars and (ii) their significant amount of gravitational binding energy, it is advantageous to translate the pulsar limit into DM's differential couplings between protons and neutrons [3,9]. While all other tests are limited to the solar neighborhood, pulsar surveys towards the galactic center (GC) [32–35] might find suitable pulsars in the future with much larger driving forces from the galactic DM distribution (in particular, the expected DM spike around the GC [36–39]) and therefore improve the bounds significantly.

Testing EP with pulsars.—The possibility to test the (strong) EP with binary pulsars was proposed by Damour and Schäfer [12], utilizing the differential acceleration from the galactic matter distribution on the two components of a binary. The relative acceleration reads $\ddot{\boldsymbol{R}} = -\mathcal{G}M\hat{\boldsymbol{R}}/R^2 + \boldsymbol{A}_{\rm PN} + \boldsymbol{A}_\eta$, where $\boldsymbol{R}$ is the relative separation, $\mathcal{G}$ denotes the effective gravitational constant, M is the total mass of the binary, $R \equiv |\boldsymbol{R}|$, and $\hat{\boldsymbol{R}} \equiv \boldsymbol{R}/R$. In the above expression, $\boldsymbol{A}_{\rm PN}$ denotes the post-Newtonian (PN) corrections [2,12,30], and we consider $\boldsymbol{A}_\eta$ as the EP-violating anomalous acceleration towards DM. At leading order, $\boldsymbol{A}_\eta = \eta_{\rm DM}^{\rm (NS,WD)}\boldsymbol{a}_{\rm DM}$ for a neutron-star–white-dwarf (NS-WD) binary [3,12,30]. It is better to view the apparent EP violation arising from a new long-range interaction (namely, fifth force) between DM and ordinary matter [9,40]. In the following, we use GR for gravity, and $\mathcal{G}$ becomes the Newtonian gravitational constant G.

We denote $\hat{\boldsymbol{a}}$ as the unit vector directing from the center of the binary towards periastron and $\hat{\boldsymbol{k}}$ as the one along orbital angular momentum. After averaging over an orbit, the secular changes on the orbital elements, introduced by the relative acceleration, are summarized as $\langle dP_b/dt\rangle = 0$, $\langle d\boldsymbol{e}/dt\rangle = \boldsymbol{f}\times\boldsymbol{l} + \dot{\omega}_{\rm PN}\hat{\boldsymbol{k}}\times\boldsymbol{e}$, and $\langle d\boldsymbol{l}/dt\rangle = \boldsymbol{f}\times\boldsymbol{e}$. We have introduced $\boldsymbol{e} \equiv e\hat{\boldsymbol{a}}$, $\boldsymbol{l} \equiv \sqrt{1-e^2}\hat{\boldsymbol{k}}$, and $\boldsymbol{f} \equiv \frac{3}{2}\mathcal{V}_O^{-1}\boldsymbol{A}_\eta$ [12,30], with P_b as the orbital period, e as the orbital eccentricity, and $\mathcal{V}_O \equiv (2\pi GM/P_b)^{1/3}$. At first PN order, the periastron advance rate reads $\dot{\omega}_{\rm PN} = 6\pi(\mathcal{V}_O/c)^2/[P_b(1-e^2)]$. Integrating the above differential equations gives the orbital dynamics, which is concisely summarized as $\boldsymbol{e}(t) = \boldsymbol{e}_{\rm PN}(t) + \boldsymbol{e}_\eta$ [12]. Graphically, the evolution of the orbital eccentricity vector $\boldsymbol{e}(t)$ has two components: (i) a general-relativistically precessing $\boldsymbol{e}_{\rm PN}(t)$ with a rate $\dot{\omega}_{\rm PN}$ and (ii) a constant "forced" eccentricity, $\boldsymbol{e}_\eta \equiv \boldsymbol{f}_\perp\dot{\omega}_{\rm PN}^{-1}$ with $\boldsymbol{f}_\perp$ as the projection of $\boldsymbol{f}$ on the orbital plane. This was used extensively to constrain the EP with binary pulsars under a probabilistic assumption on unknown angles [12–14,16,17].

Recently, a direct test, which evades the probabilistic assumption, was proposed out of this framework [30]. It uses the time derivatives of the orbital eccentricity vector $\dot{\boldsymbol{e}}$ and of the orbital inclination; the latter causes a nonzero time derivative of the projected semimajor axis $\dot{x}$. These parameters are directly fitted from the time-of-arrival (TOA) data [41]. The first implementation of the idea, based on pulsar timing data from EPTA and NANOGrav, was achieved by Zhu *et al.* [19] with PSR J1713 + 0747. Using $\dot{\boldsymbol{e}}$ of PSR J1713 + 0747 [19] and the acceleration from DM at its location [22], we obtain $|\eta_{\rm DM}^{\rm (NS,WD)}| < 0.004$ at 95% C.L.

Nongravitational forces between DM and ordinary matter.—To interpret the result from pulsar timing, we will adopt the generic framework widely used in testing the EP [3,9,20,23]. In quantum field theory, scalar or vector boson exchange introduces a spin-independent potential between a test mass A and the attractor (here the DM) [3,9,40], $V(r) = \mp\, g_5^2 q_5^{(A)} q_5^{\rm DM} e^{-r/\lambda}/4\pi r$, where g_5 is the coupling constant, q_5 is the (dimensionless) charge, and the upper (lower) sign is for the scalar (vector) boson. From the potential, one has [9]

$$\eta_{\rm DM}^{(A,B)} = \pm\frac{g_5^2}{4\pi G u^2}\frac{q_5^{\rm DM}}{\mu_{\rm DM}}\left(\frac{q_5^{(A)}}{\mu_A} - \frac{q_5^{(B)}}{\mu_B}\right)\left(1+\frac{r}{\lambda}\right)e^{-r/\lambda}, \quad (2)$$

where (q_5/μ) is an object's charge per atomic mass unit u. Hereafter, we will assume $\lambda \gg \mathcal{O}(10\ {\rm kpc})$, or equivalently, $m \ll 10^{-27}\ {\rm eV}/c^2$ for the mass of the boson field.

For test masses composed of ordinary matters (p, n, e), we parametrize the charge $(q_5/\mu) = (Z/\mu)\cos\psi + (N/\mu)\sin\psi$ [9] with the mixing angle satisfying $\tan\psi \equiv q_5^{(n)}/(q_5^{(p)} + q_5^{(e)})$. This is the most general expression for vector charge and a reasonable tree-level approximation for scalar charge [3,20]. Notice that in Eq. (2) the masses are reduced according to the objects' (negative) binding energies. For ordinary bodies, one has $(B/\mu) \equiv (Z/\mu) + (N/\mu) = 1 + \mathcal{O}(10^{-3})$; see Table I. For NSs, due to their significant gravitational binding energy, $(B/\mu) = 1 + \mathcal{O}(10^{-1})$.

In Fig. 1, we plot the constraints on the ratio of nongravitational acceleration of neutral hydrogen to the total acceleration towards the galactic DM, $a_{\rm DM}^{\rm nongrav}/a_{\rm DM}^{\rm grav}$,

TABLE I. Material sensitivities for different objects [3]. For NSs, the gravitational binding energy is assumed to be proportional to mass [19,42] and the composition is dominated by neutrons.

	Z/μ	N/μ	B/μ
Be	0.443 84	0.554 80	0.998 65
Al	0.481 81	0.518 87	1.000 68
Ti	0.459 61	0.541 47	1.001 08
Pt	0.399 84	0.600 34	1.000 18
Earth	0.49	0.51	1.00
Moon	0.50	0.50	1.00
NS (1.33 $M_\odot$)	$\simeq$0	$\simeq$1.19	$\simeq$1.19
WD (0.290 $M_\odot$)	$\simeq$0.5	$\simeq$0.5	$\simeq$1.0

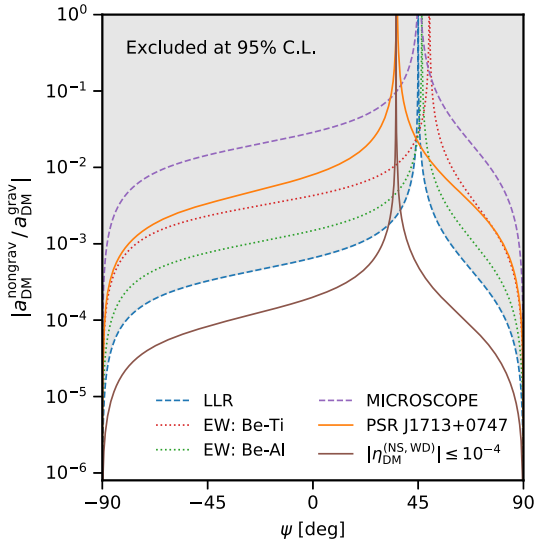

FIG. 1. The 95% C.L. limits on $|a_{\rm DM}^{\rm nongrav}/a_{\rm DM}^{\rm grav}|$ for neutral hydrogen, from LLR [27–29], Eöt-Wash (EW) experiments [9], *MICROSCOPE* [8], and PSR J1713 + 0747 [19]. The expected limit from a hypothetical NS-WD system with a 1.4 $M_\odot$ NS that constrains $|\eta_{\rm DM}^{\rm (NS,WD)}| \le 10^{-4}$ at 95% C.L. is also plotted.

as a function of the (theory-dependent) mixing angle. Although PSR J1713+0747 only limits $|\eta_{\rm DM}^{\rm (NS,WD)}| \lesssim 0.004$, the vast material difference between the NS and the WD boosts its constraint significantly. We have updated an underestimation of the galactic DM acceleration from 5×10^{-11} m s^{-2} [9,20,23] to 9.2×10^{-11} m s^{-2} [22], thus tightening the limits in Wagner *et al.* [9] even further. As we can see, because NSs' (B/μ) significantly deviates from unity, the unconstrained region differs from $\psi \simeq 45°$ for PSR J1713 + 0747, and the limit around $\psi \simeq 45°$ is given by this binary. In the following, we discuss how the proposed test will improve in the future.

DM spikes around the GC.—As stressed by Hui *et al.* [43], DM models have seldom been successfully examined by observations at scales $\lesssim$10 kpc, due to the complication of baryonic physics and unknown DM properties. Nevertheless, well-motivated models exist for the DM distribution around the GC. We consider the generalized Navarro-Frenk-White (GNFW) profile [44] augmented with DM spikes around the supermassive black hole (BH) in the GC, Sgr A* [36–39,45,46].

The Navarro-Frenk-White (NFW) profile is a common approximation to the density profile found in DM-only cosmological simulations [44]. Here we consider a generalized form

$$\rho_{\rm GNFW}(r) = \frac{\rho_0}{(r/R_s)^\gamma (1 + r/R_s)^{3-\gamma}}, \tag{3}$$

where $R_s = 20$ kpc, and ρ_0 is fixed by requiring $\rho_{\rm GNFW} = 0.4$ GeV cm^{-3} at the location of our Solar System ($r \simeq 8$ kpc). The canonical NFW profile used $\gamma = 1$; it fits the outer galactic halo well (see, e.g., McMillan [22]). We are mostly interested in the inner region of the halo, and will consider $\gamma \in [1.0, 1.4]$, motivated by numerical simulations (e.g., $\gamma \simeq 1.24$ in Diemand *et al.* [47]) and *Fermi* Large Area Telescope γ-ray observations (e.g., $\gamma \simeq 1.26$ in Daylan *et al.* [48]).

Gondolo and Silk [36] pointed out that the GNFW model cannot give an accurate description for the inner subparsec region close to the GC. In response to the adiabatic growth of Sgr A*, a DM spike with $\rho_{\rm sp}(r) \propto r^{-\gamma_{\rm sp}}$ will form, with $\gamma_{\rm sp} = (9 - 2\gamma)/(4 - \gamma)$ for collisionless DM. It forms inside the radius of gravitational influence $R_h \equiv GM_\bullet/v_0^2 \simeq 1.7$ pc of Sgr A*, where $M_\bullet \simeq 4 \times 10^6\ M_\odot$ is the mass of the BH and $v_0 \simeq 105$ km s^{-1} [49] is the one-dimensional velocity dispersion of DM in the halo outside the spike. Including GR effects [38] and the rotation of the BH [39] will further enhance the spike. Nevertheless, the maximum density of the spike is limited by the annihilation cross section of DM particles [45], producing $\rho_{\rm in}(r) \propto r^{-\gamma_{\rm in}}$ ($\gamma_{\rm in} \simeq 0.5$ for s-wave annihilation and $\gamma_{\rm in} \simeq 0.34$ for p-wave annihilation [46]). Such a weak annihilation cusp happens inside $R_{\rm in} \sim$ mpc where the density reaches the "annihilation plateau" $\rho_{\rm ann} \simeq 1.7 \times 10^8\ M_\odot\,{\rm pc}^{-3}$.

Taking the above results into consideration, we use a DM density profile

$$\rho_{\rm DM}(r) = \begin{cases} \frac{\rho_{\rm sp}(r)\rho_{\rm in}(r)}{\rho_{\rm sp}(r)+\rho_{\rm in}(r)}, & 4GM_\bullet/c^2 \le r < R_{\rm sp} \\ \rho_{\rm GNFW}(r), & r \ge R_{\rm sp} \end{cases}, \tag{4}$$

where three different values for $R_{\rm sp}$ ($= \frac{1}{5}R_h$, R_h, $5R_h$) are adopted for illustrating purposes. Normalization factors for $\rho_{\rm sp}(r)$ and $\rho_{\rm in}(r)$ are obtained by continuity.

DM density profiles at different radii are given in the upper panel of Fig. 2 for GNFW indices $\gamma \in [1.0, 1.4]$. The steepening of the DM spike (relative to the GNFW profile) happens at $r \sim 10$ pc, and its flattening happens at $r \sim 10^{-2}$ pc ($R_{\rm in} = 2.7$, 5.9, and 13 mpc for the three $R_{\rm sp}$'s when $\gamma = 1.2$) [37]. In the lower panel, we give the acceleration produced solely by the DM, $a_{\rm DM}(r) \equiv G\int^r 4\pi r'^2 \rho_{\rm DM}(r')dr'/r^2$. One can see that, $a_{\rm DM}(r)/a_{\rm DM}^\odot \le 1.1$ at the location of PSR J1713 + 0747 [19], where $a_{\rm DM}^\odot$ is the DM acceleration at the Solar System. However, at the location of the magnetar PSR J1745 − 2900 ($r \sim 0.1$ pc) [50], depending on the value of γ, this quantity can be as high as 23–870 for $R_{\rm sp} = \frac{1}{5}R_h$, 180–3600 for $R_{\rm sp} = R_h$, and 1400–14 000 for $R_{\rm sp} = 5R_h$. This factor will be the *gain* in the driving force to test the universality of free fall (UFF) towards DM if a binary pulsar is found there.

Pulsar surveys towards the GC.—The magnetar PSR J1745 − 2900 [50] is already within the most interesting region, but unfortunately it is not in a binary. The closest binaries known so far are PSRs J1755 − 2550 and

J1759 − 24, with radial distances from the GC of about 2 kpc, although the exact distances are still highly uncertain [51,52]. Future radio surveys are likely to overcome existing selection effects and promise to find binaries in much closer proximity. In particular, the Square Kilometre Array (SKA) has the capability of finding nearly all radio pulsars beamed towards Earth [53], including those pulsars near the GC [34]. Already, the first phase, SKA1, should find about 10 000 pulsars [54] in the Galaxy, about 10% of which can be expected to be in binaries, based on the currently known population. In order to probe the GC region, high-frequency surveys may be needed to overcome the scattering of the radio pulses in the turbulent interstellar medium [41], but such surveys are ongoing already and more are planned [55]. Constraints on the pulsar population from observations at multiwavelengths around the GC [33] suggest that the inner parsec of the Galaxy could harbor as many as $\sim 10^3$ active radio pulsars that are beaming toward the Earth. Those pulsars should include a number of suitable binaries, and simulations show that even a few PSR-BH systems should be present in the central parsec today [57], which would be prime targets for the studies suggested here.

Discussions.—In this Letter, we propose to use radio timing of binary pulsars to constrain nongravitational forces between DM and ordinary matter that will appear as an apparent violation of the EP towards DM. As we can see in Fig. 1, the current limit on UFF from PSR J1713 + 0747 [19] is already providing important improvement over current best limits [9,27]. The test with pulsars has unique advantages over other tests, which we will recapitulate and further elaborate below.

Driving force: Driving force sets an important reference in testing the EP. At the site of the Eöt-Wash laboratory in Seattle, the driving forces from Earth, the Sun, and DM are 1.68×10^{-2}, 5.9×10^{-3}, and 9.2×10^{-11} m s^{-2}, respectively; thus, the 1σ limits (from the Be-Ti pair) are $|\eta_\oplus| \lesssim 2 \times 10^{-13}$, $|\eta_\odot| \lesssim 5 \times 10^{-13}$, and $|\eta_{\rm DM}| \lesssim 3 \times 10^{-5}$ [9]. To test $\eta_\oplus$, *MICROSCOPE* gains a factor of 500 in the driving force by putting the experiment in space [8]. However, it does not have such a gain when the attractor is DM. For the same reason, the triple pulsar [58,59], while gaining a factor of $\mathcal{O}(10^7)$ in driving force to test the strong EP, cannot probe the UFF towards DM at a comparable level. As shown in Fig. 2, if future surveys find suitable binary pulsars within $\mathcal{O}(10$ pc$)$ of the GC, the driving force can easily be enhanced by orders of magnitude.

Measurement precision: Freire *et al.* [30] showed that uncertainties in $\dot{e}$ and $\dot{x}$ (denoted as $\delta\dot{e}$ and $\delta\dot{x}$) scale as $\delta\dot{e} \simeq 8.0\delta t/x\sqrt{\bar{N}T^3}$ and $\delta\dot{x} \simeq 5.3\delta t/\sqrt{\bar{N}T^3}$, where $\bar{N}$ is the average number of TOAs per unit time, δt is the rms of TOA residuals, and T is the observing baseline. Even with current pulsars, longer observations will improve the test as $T^{-3/2}$, and future telescopes, like the Five Hundred Metre Aperture Spherical Telescope [60] and SKA [31,53], will

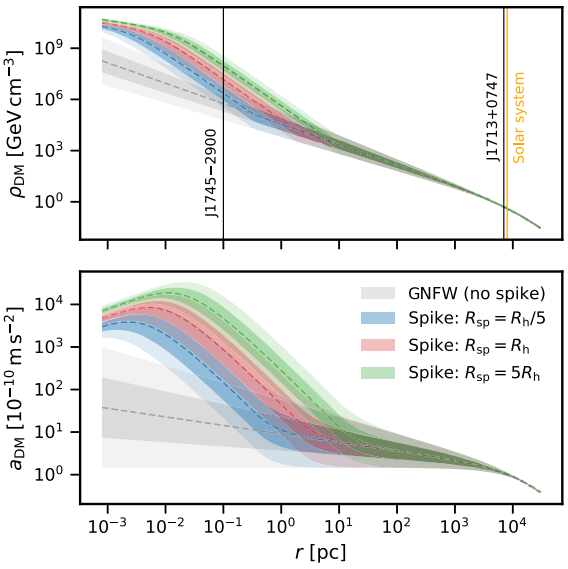

FIG. 2. (Upper) DM density as a function of the distance to the GC. (Lower) Acceleration produced by the DM inside radius r. The lighter and darker shadowed regions enclose $\gamma \in [1.0, 1.4]$ and $\gamma \in [1.1, 1.3]$, respectively, while the dashed lines give $\gamma = 1.2$. (Upper) Locations of PSR J1745 − 2900 [50], PSR J1713 + 0747 [19], and the Solar System are indicated.

be able to improve the timing precision δt significantly. Therefore, the proposed test will improve continuously. In addition, it was shown that the $\dot{\boldsymbol{e}}$ test is a clean test, not being contaminated by external effects [30].

Material sensitivity: NSs are unique in the sense that they contain a dominant portion of neutron-rich materials. This gains a factor of $\mathcal{O}(10^2)$ for most ψ's when interpreting the $\eta_{\rm DM}$ limit in Fig. 1. Depending on the equation of state, NSs might contain exotic excitations like pions and kaons. It would allow us to test couplings of DM with these d.o.f. that are inaccessible with other alike experiments.

Binding energy: As ordinary matter has $(B/\mu) \simeq 1$, any individual experiment will have an infinite peak around $\psi \simeq 45°$ in Fig. 1. This infinite peak can be removed by combining results from two or more different test-body pairs. Because of the significant gravitational binding energy of NSs, the peak is shifted towards smaller $\psi \simeq \tan^{-1}(1 - 2\epsilon)$, where ϵ is the (absolute value of) fractional gravitational binding energy. The combination of our limits from pulsar timing with existing experiments gives an improved constraint in the region around $\psi \simeq 45°$. Future results from other pulsar binaries close to the GC have the possibility of making substantial improvements over most of the range of the ψ parameter (see Fig. 1).

It is pleasing to see that pulsar timing naturally possesses all the advantages mentioned above to boost its test of UFF towards DM. Although a binary pulsar at the GC will most certainly not have the same timing precision as PSR J1713 + 0747, due to the boost in the driving force by orders of magnitude, it might still allow for a limit of

$|\eta_{\rm DM}^{\rm (NS,WD)}| \lesssim 10^{-4}$. In Fig. 1, we plot the corresponding constraint, which will exclude nongravitational force between DM and neutral hydrogen at 1‰ level for any mixing angle.

We are grateful to Ralph Eatough, Paulo Freire, and Anna Nobili for discussions and to the anonymous referees for comments that improved the manuscript. We acknowledge financial support by the European Research Council (ERC) for the ERC Synergy Grant BlackHoleCam under Contract No. 610058.

*lshao@mpifr-bonn.mpg.de

[1] I. Newton, *Philosophiae Naturalis Principia Mathematica* (Streater, London, 1687).
[2] C. M. Will, *Theory and Experiment in Gravitational Physics* (Cambridge University Press, Cambridge, England, 1993).
[3] E. G. Adelberger, J. H. Gundlach, B. R. Heckel, S. Hoedl, and S. Schlamminger, Prog. Part. Nucl. Phys. **62**, 102 (2009).
[4] C. M. Will, Living Rev. Relativity **17**, 4 (2014).
[5] A. M. Nobili and A. Anselmi, Phys. Lett. A, DOI: 10.1016/j.physleta.2017.09.027 (2017).
[6] V. Fock and N. Kemmer, *Theory of Space, Time and Gravitation* (Pergamon Press, Oxford, England, 1964).
[7] T. Damour, Classical Quantum Gravity **29**, 184001 (2012).
[8] P. Touboul *et al.*, Phys. Rev. Lett. **119**, 231101 (2017).
[9] T. A. Wagner, S. Schlamminger, J. H. Gundlach, and E. G. Adelberger, Classical Quantum Gravity **29**, 184002 (2012).
[10] J. G. Williams, S. G. Turyshev, and D. Boggs, Classical Quantum Gravity **29**, 184004 (2012).
[11] K. Nordtvedt, Phys. Rev. **169**, 1017 (1968).
[12] T. Damour and G. Schäfer, Phys. Rev. Lett. **66**, 2549 (1991).
[13] N. Wex, Astron. Soc. Pac. Conf. Ser. **202**, 113 (2000).
[14] I. H. Stairs *et al.*, Astrophys. J. **632**, 1060 (2005).
[15] M. E. Gonzalez *et al.*, Astrophys. J. **743**, 102 (2011).
[16] W. W. Zhu *et al.*, Astrophys. J. **809**, 41 (2015).
[17] N. Wex, in *Frontiers in Relativistic Celestial Mechanics: Applications and Experiments*, edited by S. M. Kopeikin (Walter de Gruyter GmbH, Berlin, 2014), Vol. 2, p. 39.
[18] L. Shao and N. Wex, Sci. China Phys. Mech. Astron. **59**, 699501 (2016).
[19] W. W. Zhu *et al.*, arXiv:1802.09206.
[20] C. W. Stubbs, Phys. Rev. Lett. **70**, 119 (1993).
[21] P. W. Graham, D. E. Kaplan, J. Mardon, S. Rajendran, and W. A. Terrano, Phys. Rev. D **93**, 075029 (2016).
[22] P. J. McMillan, Mon. Not. R. Astron. Soc. **465**, 76 (2017).
[23] G. Smith, E. G. Adelberger, B. R. Heckel, and Y. Su, Phys. Rev. Lett. **70**, 123 (1993).
[24] Y. Su, B. R. Heckel, E. G. Adelberger, J. H. Gundlach, M. Harris, G. L. Smith, and H. E. Swanson, Phys. Rev. D **50**, 3614 (1994).
[25] Y. Su, B. R. Heckel, E. G. Adelberger, J. H. Gundlach, M. Harris, G. L. Smith, and H. E. Swanson, Phys. Rev. D **51**, 3135 (1995).
[26] K. L. Nordtvedt, Astrophys. J. **437**, 529 (1994).
[27] K. L. Nordtvedt, J. Müller, and M. Soffel, Astron. Astrophys. **293**, L73 (1995).
[28] J. D. Anderson, M. Gross, K. L. Nordtvedt, and S. G. Turyshev, Astrophys. J. **459**, 365 (1996).
[29] J. G. Williams, S. G. Turyshev, and D. H. Boggs, Int. J. Mod. Phys. D **18**, 1129 (2009).
[30] P. C. C. Freire, M. Kramer, and N. Wex, Classical Quantum Gravity **29**, 184007 (2012).
[31] L. Shao *et al.*, Proc. Sci., AASKA14 (**2015**) 042.
[32] J.-P. Macquart, N. Kanekar, D. A. Frail, and S. M. Ransom, Astrophys. J. **715**, 939 (2010).
[33] R. S. Wharton, S. Chatterjee, J. M. Cordes, J. S. Deneva, and T. J. W. Lazio, Astrophys. J. **753**, 108 (2012).
[34] R. P. Eatough *et al.*, Proc. Sci., AASKA14 (**2015**) 045.
[35] M. De Laurentis, Z. Younsi, O. Porth, Y. Mizuno, and L. Rezzolla, Phys. Rev. D **97**, 104024 (2018).
[36] P. Gondolo and J. Silk, Phys. Rev. Lett. **83**, 1719 (1999).
[37] B. D. Fields, S. L. Shapiro, and J. Shelton, Phys. Rev. Lett. **113**, 151302 (2014).
[38] L. Sadeghian, F. Ferrer, and C. M. Will, Phys. Rev. D **88**, 063522 (2013).
[39] F. Ferrer, A. M. da Rosa, and C. M. Will, Phys. Rev. D **96**, 083014 (2017).
[40] E. Fischbach, D. Sudarsky, A. Szafer, C. Talmadge, and S. H. Aronson, Phys. Rev. Lett. **56**, 3 (1986); **56**, 1427(E) (1986).
[41] D. R. Lorimer and M. Kramer, *Handbook of Pulsar Astronomy* (Cambridge University Press, Cambridge, England, 2005).
[42] T. Damour and G. Esposito-Farèse, Classical Quantum Gravity **9**, 2093 (1992).
[43] L. Hui, J. P. Ostriker, S. Tremaine, and E. Witten, Phys. Rev. D **95**, 043541 (2017).
[44] J. F. Navarro, C. S. Frenk, and S. D. M. White, Astrophys. J. **490**, 493 (1997).
[45] E. Vasiliev, Phys. Rev. D **76**, 103532 (2007).
[46] S. L. Shapiro and J. Shelton, Phys. Rev. D **93**, 123510 (2016).
[47] J. Diemand, M. Kuhlen, P. Madau, M. Zemp, B. Moore, D. Potter, and J. Stadel, Nature (London) **454**, 735 (2008).
[48] T. Daylan, D. P. Finkbeiner, D. Hooper, T. Linden, S. K. N. Portillo, N. L. Rodd, and T. R. Slatyer, Phys. Dark Universe **12**, 1 (2016).
[49] K. Gultekin *et al.*, Astrophys. J. **698**, 198 (2009).
[50] R. P. Eatough *et al.*, Nature (London) **501**, 391 (2013).
[51] C. Ng *et al.*, Mon. Not. R. Astron. Soc. **450**, 2922 (2015).
[52] C. Ng *et al.*, Mon. Not. R. Astron. Soc. **476**, 4315 (2018).
[53] M. Kramer, D. C. Backer, J. M. Cordes, T. J. W. Lazio, B. W. Stappers, and S. Johnston, New Astron. Rev. **48**, 993 (2004).
[54] E. F. Keane *et al.*, Proc. Sci., AASKA14 (**2015**) 040 [arXiv:1501.00056].
[55] C. Goddi *et al.*, Int. J. Mod. Phys. D **26**, 1730001 (2017).
[57] C.-A. Faucher-Giguère and A. Loeb, Mon. Not. R. Astron. Soc. **415**, 3951 (2011).
[58] S. M. Ransom *et al.*, Nature (London) **505**, 520 (2014).
[59] L. Shao, Phys. Rev. D **93**, 084023 (2016).
[60] R. Nan, D. Li, C. Jin, Q. Wang, L. Zhu, W. Zhu, H. Zhang, Y. Yue, and L. Qian, Int. J. Mod. Phys. D **20**, 989 (2011).